X CONGRESSO NACIONAL DE ENGENHARIA MECÂNICA 2018
20 A 24 DE MAIO DE 2018 SALVADOR – BA – BRASIL

Influence of tool geometry and process velocities on torque in friction stir welding

Karen Johanna Quintana, kjq.cuellar@mecanica.coppe.ufrj.br[1]
Jose Luis Silveira, jluis@mecanica.ufrj.br[2]

[1]Universidade Federal do Rio de Janeiro, Department of Mechanical Engineering, COPPE, RJ, Brazil, Cidade Universitária, Ilha do Fundão, Centro de Tecnologia, Bloco G, Sala 204
[2]Universidade Federal do Rio de Janeiro, Department of Mechanical Engineering, POLI and COPPE, RJ, Brazil, Cidade Universitária, Ilha do Fundão, Centro de Tecnologia, Bloco G, Sala 204

Abstract: *Torque is a fundamental process quantity in FSW because it is related to weld quality, process control, and mechanical properties of the weld. However, models and experimental studies to determine the influence of the tool geometry and all the process velocities on torque have received little attention. In this paper, the influence of the pin and shoulder on the torque is individually considered. The torque was measured during FSW experiments for different combinations of the tool geometry and the process velocities and a model to describe the torque as a function of the main welding parameters was proposed. The results showed a strong influence of the tool geometry on torque and a good agreement between the experimental data and the model.*

Keywords: *Friction Stir Welding, Torque behaviour, Tool geometry, FSW experiments, FSW velocities*

1. INTRODUCTION

Friction stir welding is a solid-state welding technique mainly developed to weld materials with poor weldability such as aluminum, magnesium, copper, and other light alloys (Mishra and Ma, 2005; Mahoney *et al.*, 1998). During the FSW, the material does not reach the melting temperature to produce the weld, in this process, a rotating tool maintains a constant rotational speed, penetrates the weld material and advances to produce the weld. The friction at the tool-material interface produced by the constant rotation of the tool increases the local temperature of the material and, consequently, the material around the tool is softened, plastically deformed, and stirred by the tool rotation to produce the weld. The absence of material melting produces welds with better quality and properties than by the conventional fusion techniques. Moreover, the process is simpler, requires less energy is cost-efficient and environmentally friendly (Rhodes *et al*., 1997; Rajakumar *et al*., 2011; Qian *et al*., 2012). The main process variables in FSW are the tool geometry and the rotational, plunging, and welding speeds. Currently, FSW is used to weld different types of materials as ferrous, non-ferrous, polymers, and dissimilar materials (Nandan *et al*., 2008) and it has evolved to variations such as Friction Stir Spot Welding (FSSW), to obtain spot welds (Mahoney *et al.*, 1998), and Friction Stir Processing (FSP) to modify material properties at the surface (Mishra and Ma, 2005).

By the conditions of the FSW process, during the welding the tool is submitted to a torque and three forces, the axial, welding, and transverse forces. These quantities are important in the FSW process to the process control, adequate tool design, to determine the FSW machine capacity required to weld an specific material, and to the weld quality (Quintana and Silveira, 2018). Torque in FSW process is closely related to the temperature in the stir zone, material state, weld quality, and it is fundamental to the process control and tool design (Nandan *et al*., 2008). Torque is related to the temperature in the process through the local stress. For high temperatures, the local stress of the material decreases and, consequently, the torque also decreases (Yan *et al*., 2005; Upadhyay and Reynolds, 2010). Moreover, the torque is useful to the process control and to the proper selection of the equipment to perform the FSW. The signal of torque during the FSW process allows detecting the different phases in the FSW process (Cui *et al*., 2010; Kumar *et al*., 2012). The torque multiplied by the rotational speed has been used for some authors (Khandkar *et al*., 2003; Schmidt *et al*., 2004; Cui *et al*., 2010; Pew *et al.*, 2007) to compute the power in the FSW process.

Torque is mainly influenced by the welding and rotational speeds, tool geometry, plunging depth, and material properties. Some experimental studies (Cui *et al*., 2010; Long *et al.*, 2007; Upadhyay and Reynolds, 2010) showed that the torque decreases with higher rotational speeds and conversely increases with higher welding speeds. Quintana and Silveira (2017a) measured the torque during FSW experiments for different combinations of welding and rotational speeds. Based on the experimental results and the analysis of variance (ANOVA), the authors founded that although the

influence of the welding speed on the torque is considerably smaller than the influence of the rotational speed, the torque behavior is influenced by the interaction of both speeds. Additionally, the authors adjusted an experimental torque model via inverse problem method, and using experimental data from literature founded an influence of the tool geometry on the torque behavior. Khandkar *et al.* (2003) and Schmidt *et al.* (2004) determined that the tool geometry and the properties of the weld material affect the torque value.

Although several authors had studied the torque as a function of the tool geometry and the rotational and welding speeds, the contribution of each part of the tool and the plunging speed on the torque during the two phases of the FSW process, the plunging and the welding, have not been determined. With the goal of advancing the understanding of fundamental mechanics of the FSW process, in this paper, the influence of the pin and shoulder of the tool on the torque in the plunging and welding phases is separately evaluated for different plunging, rotational, and welding speeds. A mechanistic model to describe the torque as a function of the rotational and welding speed is proposed using the inverse problem methodology and the experimental data as input.

2. EXPERIMENTAL PROCEDURE

The welds were carried out in a computer numerical control (CNC) machining center adapted to the FSW process. A fixture device was designed to guarantee a suitable arrangement of the specimens during the process. A Kistler 9272 dynamometer and a multichannel charge amplifier Kistler 5070 were used to measure the torque and for the signal conditioning, respectively. Aluminum alloy AA 5052-H34 specimens with a thickness of 5mm were prepared at different levels of rotational, plunging, and welding speeds. For each set of parameters, three replicas were performed. To evaluate separately the influence of the shoulder and pin on the torque, three experimental designs were proposed. The tool material for the first and second experimental design is 1045 steel and for the third experimental design is H13 steel, heat treated to an average hardness of 50 HRC.

The first experimental design consists in the plunging of the tool into the material with a tool composed only of a pin at different levels of rotational and welding speed and several pin diameters. The welding phase is not considered in this experimental design. The experiments were carried out at four levels of rotational speed: 600, 900, 1200 and 1500 rpm, three levels of plunging speed: 4, 6, and 8 mm/min and four levels of pin diameter: 4.5, 5, 5.5, and 6 mm.

The second experimental design consists in the plunging of the tool into the material with a tool composed only by shoulder at different levels of rotational speed and several pin diameters with a plunging speed of 4 mm/min. The experiments were performed at four levels of rotational speed: 600, 900, 1200, and 1500 rpm and three levels of shoulder diameter: 8, 10, and 12 mm. A total plunging depth of 0.3 mm was used for all the experiments. Owing to the small plunging depth and to facilitate the data acquisition, a dwell time of 40 s was used.

The third experimental design comprises all the phases of the welding process, the plunging and the welding phases, with a complete tool composed by a shoulder diameter of 10 mm and a pin diameter of 4mm. The experiments were conducted at four levels of rotational speed: 600, 900, 1200, and 1500 rpm and three levels of welding speed: 100, 200, and 300 mm/min. A total plunging depth of 4.1 mm and a plunging speed of 8 mm/min were used for all the experiments.

3. EXPERIMENTAL RESULTS

3.1. Torque for the first experimental design

Figure 1a shows the torque data as a function of the rotational speed for all the evaluated plunging speeds and a pin diameter of 4.5 mm. A similar behavior was observed for all the pin diameters. The experimental results show a higher influence of the rotational speed than the plunging speed on the torque. However, an interaction between the plunging and the rotational speed on the torque is observed. For higher rotational speeds the influence of the plunging speed decreases. The heat input into the process increases with higher rotational speeds, and under this condition, the local temperature is higher, the material is more softened and, consequently, the local stress and the torque decrease. Figure 1b shows the torque data as a function of the rotational speed obtained for all the evaluated pin diameters and a plunging speed of 6 mm/min. The results indicate that in general the torque increases with the increase of the pin diameter due to the increase of the contact area at the tool-material interface. However, the influence of the pin diameter on the torque depends on the rotational speeds, for lower rotational speeds the pin diameter has a more significant influence on the torque.

The analysis of variance (ANOVA) presented in Tab. 1 confirms these two interactions between the factors of the first experimental design. The results indicate that for a statistic F of 2.38 and a *p*-level of 0.0177, there is an interaction between the effects of rotational speed and pin diameter factors on the torque. And for a statistic F of 5.91 and a *p*-level of 0.000, the ANOVA indicates that exist an interaction between the effects of rotational and plunging speeds factors on the torque.

Figure 2 shows the fitted curve of torque as a function of the rotational speed for a pin diameter of 4.5 mm and a plunging speed of 8 mm/min. This trend was observed for all the evaluated pin diameters. Table 2 presents the fitted equations for the torque at each plunging speed and all pin diameters. In accordance to the behavior observed in Fig 1, the fitted equation is a downward exponential function for the torque as a function of the rotational speed.

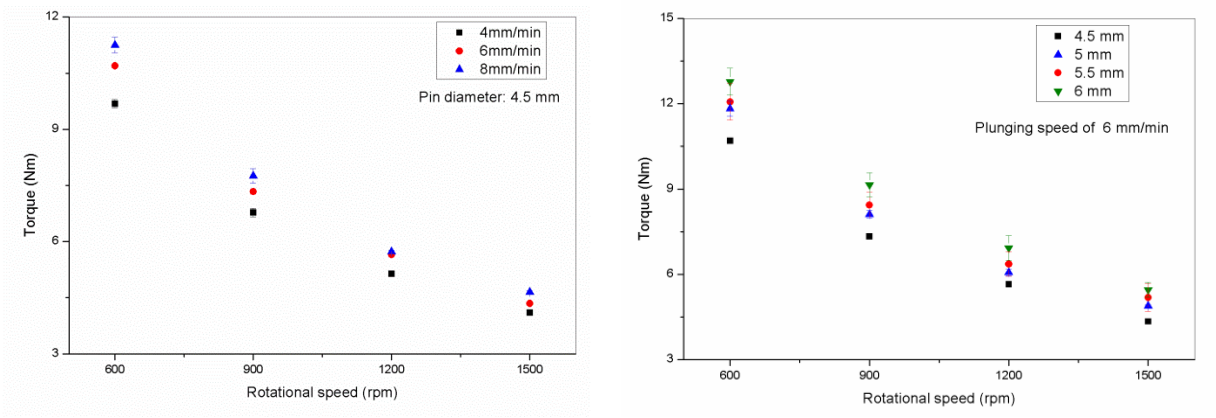

a) b)

Figure 1. Torque as a function of rotational speed for: a) a pin diameter of 4.5 mm and all plunging speeds, and b) all the evaluated pin diameters and a plunging speed of 6 mm/min.

Table 1. Analysis of variance (ANOVA) for the first experimental design.

Source	Sum of square	Degree of freedom	Mean square	F	*p*-level
ω	943.19	3	314.397	1961.5	0
v_p	33.87	2	16.933	105.64	0
d_p	49.54	3	16.513	103.02	0
$\omega \cdot v_p$	5.68	6	0.947	5.91	0
$\omega \cdot d_p$	3.43	9	0.382	2.38	0.0177
$v_p \cdot d_p$	0.33	6	0.056	0.35	0.9095
$\omega \cdot v_p \cdot d_p$	2.32	18	0.129	0.8	0.6907
Erro	15.39	96	0.16		
Total	1053.76	143			

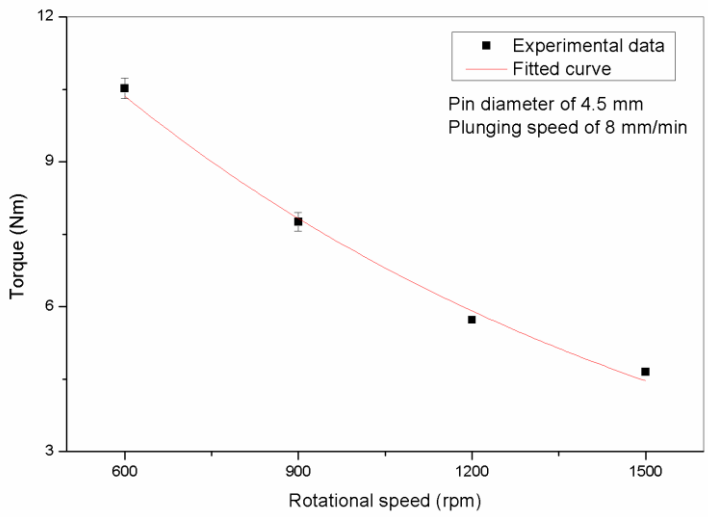

Figure 2. Fitted curve of torque for a pin diameter of 4.5 mm and a plunging speed of 8 mm/min

Table 2. Fitted curve equations of torque for the first experimental design.

Pin diameter (mm)	Plunging speed (mm/min)	Fitted curve equation for torque (Nm)	Data fitting correlation (R^2)
4.5	4	$M = 16.559e^{-1\times10^{-3}\omega}$	0.990
	6	$M = 18.684e^{-1\times10^{-3}\omega}$	0.990
	8	$M = 19.525e^{-1\times10^{-3}\omega}$	0.984
5	4	$M = 20.063e^{-1\times10^{-3}\omega}$	0.988
	6	$M = 20.376e^{-9\times10^{-4}\omega}$	0.985
	8	$M = 22.193e^{-1\times10^{-3}\omega}$	0.994
5.5	4	$M = 17.519e^{-9\times10^{-4}\omega}$	0.990
	6	$M = 20.443e^{-1\times10^{-3}\omega}$	0.985
	8	$M = 23.265e^{-1\times10^{-3}\omega}$	0.989
6	4	$M = 18.967e^{-9\times10^{-4}\omega}$	0.994
	6	$M = 21.945e^{-9\times10^{-4}\omega}$	0.994
	8	$M = 22.502e^{-9\times10^{-4}\omega}$	0.984

3.2. Torque for the second experimental design

Figure 3a shows the stabilized torque data as a function of the rotational speed for all the evaluated shoulder diameters. The torque value decreases for higher rotational speeds and increases for higher shoulder diameters. However, the influence of the rotational speed on the torque depends on the shoulder diameter, for higher shoulder diameters, the rotation speed has a greater influence on the torque value. Owing to the low plunging depth of the tool in this experimental design, a reduction in the shoulder diameter decreases significantly the contact area between the tool and the material, therefore, a smaller quantity of material is affected and both, the torque value and the influence of the rotational speed on the torque, are smaller. The analysis of variance presented in Tab. 3 indicates that for a statistic F of 14.84 and a *p*-level of 0.0, there is an interaction between the effects of the shoulder diameter and rotational speed factors on the torque value.

Figure 3b shows the fitted curve of torque as a function of the rotational speed for a shoulder diameter of 12 mm. This trend was observed for all the evaluated shoulder diameters. Table 4 presents the fitted equations for the torque as a function of the rotational speed at each shoulder diameter. For this experimental design, the more accurate description for the experimental data is a logarithmic function for the torque as a function of the rotational speed.

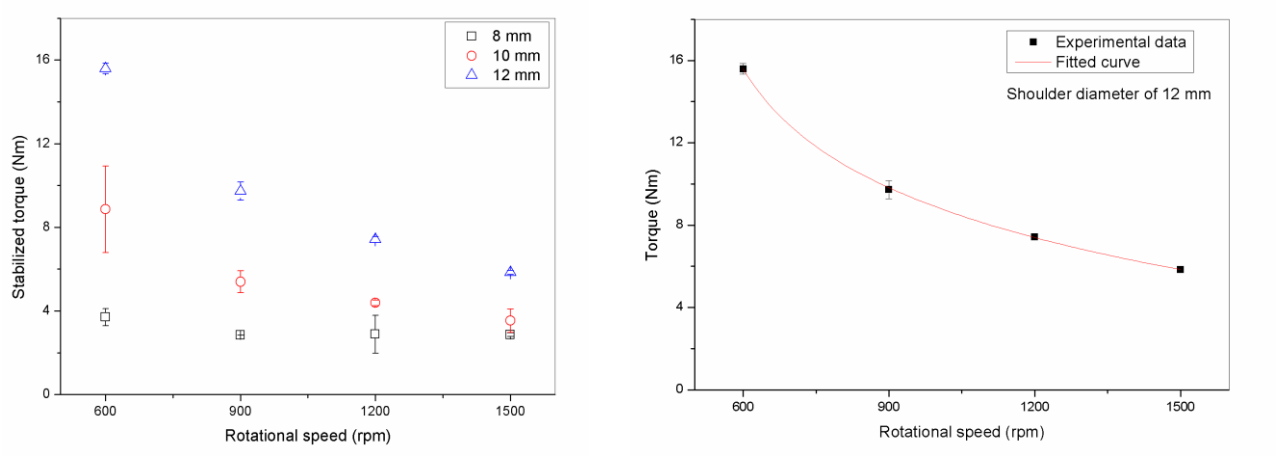

a) b)

Figure 3. a) Torque as a function of rotational speed for all the shoulder diameters and b) fitted curve for torque for a shoulder diameter of 12 mm.

Table 3. Analysis of variance (ANOVA) for the second experimental design.

Source	Sum of square	Degree of freedom	Mean square	F	*p*-level
ω	146.833	3	48.944	63.8	0
d_s	264.076	2	132.038	172.1	0
$\omega \cdot d_s$	68.307	6	11.384	14.84	0
Erro	18.417	24	0.767		
Total	497.629	35			

Table 4. Fitted curve equations of torque for the second experimental design.

Shoulder diameter (mm)	Fitted curve equation for torque (Nm)	Data fitting correlation (R^2)
8	$M = -0.881 \ln(\omega) + 9.153$	0.761
10	$M = -5.757 \ln(\omega) + 45.271$	0.950
12	$M = -10.640 \ln(\omega) + 83.069$	0.970

3.3. Torque for the third experimental design

The torque data as a function of the rotational speed during the plunging and welding phases, for all welding speeds are presented in Fig. 4a. In both phases, the torque decreases with the increase of the rotational speed; however, the torque increases with the increase of the welding speed only during the welding phase since the welding speed acts in the process exclusively during the welding phase. The high heat input produced by higher rotational speeds softens the material around the tool and decreases the local yield stress and, consequently, the torque value and the influence of the welding speed on the torque are smaller. The analysis of variance presented in Tab. 5 confirms the influence of the interaction between the rotational and the welding speeds on the torque during the welding phase, for a statistic F of 3.29 and a *p*-level of 0.0167. On the other hand, during the plunging phase, the analysis of variance indicates that, for a statistic F of 1209.61 and a *p*-level of 0, the rotational speed has influence on the torque while the welding speed, for a statistic F of 0.33 and a *p*-level of 0.723 does not present influence on the torque.

The fitted curve of torque as a function of the rotational speed for a welding speed of 100 mm/min in the welding phase is presented in Fig. 4b. This trend was observed for all the evaluated welding speeds in both, plunging and welding phases. The fitted equations for the torque as a function of the rotational speed at each welding speed, during the plunging and welding phases, are presented in Tab. 6. For all cases, the fitted equation is a downward exponential function for the torque as a function of the rotational speed.

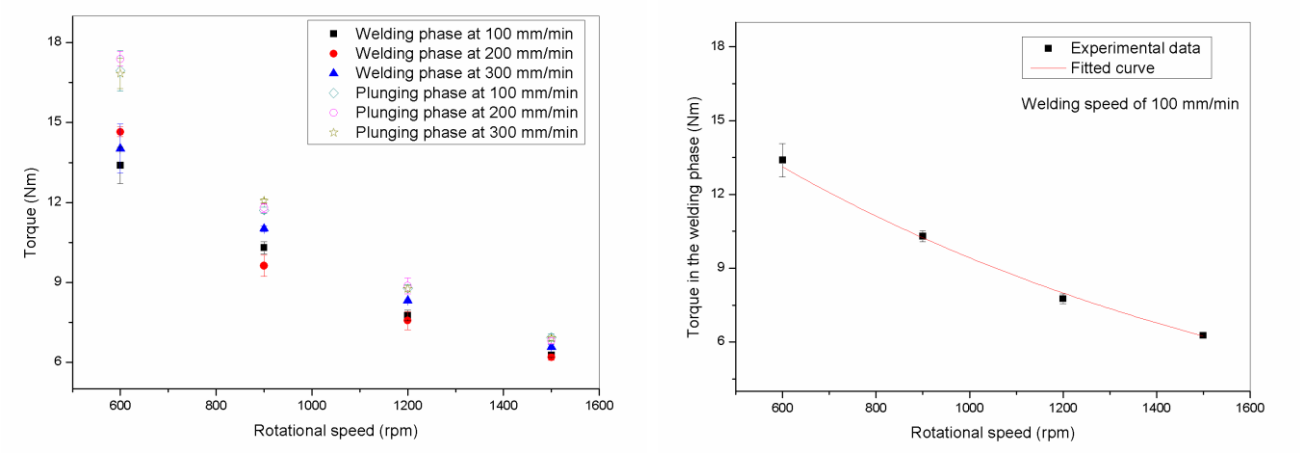

a) b)

Figure 4. a) Torque as a function of rotational speed for all the welding speeds in plunging and welding phases and b) fitted curve for torque in the welding phase for a welding speed of 100 mm/min.

Table 5. Analysis of variance (ANOVA) for the third experimental design in the plunging and welding phases.

Source	Sum of square	Degree of freedom	Mean square	F	*p*-level
Plunging phase					
ω	532.387	3	177.462	1209.61	0
v_w	0.096	2	0.048	0.33	0.723
$\omega \cdot v_w$	0.67	6	0.112	0.76	0.6074
Erro	3.521	24	0.147		
Total	536.657	35			
Welding phase					
ω	302.802	3	100.934	465.3	0
v_w	2.166	2	1.083	4.99	0.0154
$\omega \cdot v_w$	4.277	6	0.713	3.29	0.0167
Erro	5.206	24	0.217		
Total	314.451	35			

Table 6. Fitted curve equations of torque for the third experimental design.

Welding speed (mm/min)	Fitted curve equation for torque plunging phase (Nm)	Data fitting correlation (R^2)	Fitted curve equation for torque welding phase (Nm)	Data fitting correlation (R^2)
100	$M = 30.298e^{-1\times10^{-3}\omega}$	0.992	$M = 22.195e^{-9\times10^{-4}\omega}$	0.997
200			$M = 24.231e^{-9\times10^{-4}\omega}$	0.968
300			$M = 23.435e^{-9\times10^{-4}\omega}$	0.999

4. MECHANISTIC TORQUE MODEL

The maximum torque in the plunging phase of the FSW process for a complete tool is defined by Eq. (1) as the sum of two contributions, the contribution of the local shear yield stress of the material multiplied by a geometric factor, which considers the tool geometry and the contribution of the welding speed. In Eq. (1), M_p (Nm) is the maximum torque value, τ_l (Pa) is the local shear yield stress of the material, G (m^3) is a geometric factor, v_p (mm/min) is the plunging speed and C (Nm.min/mm) is a parameter estimated by inverse problem technique.

$$M_p = \tau_l G + C v_p \tag{1}$$

Owing to the close relation between the rotational speed and the local temperature in the material, the local shear yield stress τ_l considers the effect of the heat input in the process by means of the rotational speed. The temperature affects the local yield stress of the material and consequently the torque is also affected. According to Hussein *et al.* (2015) the rotational speed is the main factor that promotes the growth of temperature. Pew *et al.* (2007) correlated the heat input in the FSW process with the rotational and welding speeds and found that the heat input in the process increases significantly with higher rotational speeds. Based on the experimental results observed in Fig. 4, the local shear yield stress is described by Eq. (2) as an exponential decay function with the rotational speed. The parameters A and B in Eq. (2) will be estimated via inverse problem and described in the next section.

$$\tau_l = A e^{-B\omega} \tag{2}$$

The geometry factor G considers the contribution of the tool-material interface as given by Eq. (3), where h_p is the pin height, r_p is the pin radius and r_s is the shoulder radius.

$$G = \int_0^{r_S}\int_0^{2\pi} r\left(rd\theta dr\right) + \int_0^{h_P}\int_0^{2\pi} r\left(rd\theta dl\right) + \int_0^{r_P}\int_0^{2\pi} r\left(rd\theta dr\right) \tag{3}$$

The torque M_w (Nm) in the welding phase of the process is described by Eq. (4) as a function of the maximum torque in the plunging phase and the contribution of the welding speed v_w (mm/min) multiplied by the parameter D. The parameter D considers the contribution of the rotational speeds during the welding phase and is described by Eq. (5) where the parameters D_1 (Nm/(mm/min)) and D_2 (rpm^{-1}) are estimated via inverse problem and described in the next section.

$$M_W = M_p + D v_W \tag{4}$$

$$D = D_1 e^{-D_2\omega} \tag{5}$$

4.1. Estimation of parameters

The inverse problem method used to estimate the model parameters followed the procedure previously described by Quintana and Silveira (2017a). The D-optimum design was used to select the optimal maximum rotational speed, and the number of measurements for estimating the parameters by means of the variable and fixed frequency analysis, respectively. The Levenberg-Marquardt iterative method was implemented to estimate the parameters using the experimental data as input. All the parameters were evaluated to be estimated via inverse problem, and when possible they were estimated via inverse problem. The parameters that could not be estimated via inverse problem were obtained from the experimental data. All the parameters were described as a function of the evaluated factors in the experimental designs. The equations for each parameter were obtained from the estimated values for each combination of factors as described in detail in Quintana and Silveira (2017b). For the torque model in the plunging phase, the parameters A and B from Eq. (2) are described as a function of the contact area at the tool-material interface a_c (mm^2) and the plunging speed v_p as presented in Eq. (6) and (7), respectively. The parameter C from Eq. (1) is given by the Eq. (8) as a function of the contact area.

$$A = (-4.523\times10^{7} v_p + 6.018\times10^{8}) e^{(2.37\times10^{3} v_p - 2.724\times10^{4}) a_c} \tag{6}$$

$$B = -(0.481) a_c v_p + (4.176) a_c + 3.95 \tag{7}$$

$$C = (9.485\times10^{2}) a_c - 0.100 \tag{8}$$

For the torque model in the welding phase, the parameters D_1 and D_2 from Eq. (5) are described as a function of the welding speed by Eq. (9) and (10), respectively.

$$D_1 = (1.967 \times 10^{-4}) v_w - 0.068 \tag{9}$$

$$D_2 = -(1.211 \times 10^{-6}) v_w - 0.0014 \tag{10}$$

4.2. Model calibration

Figure 5 shows the comparison of the torque value obtained experimentally and by the model for the plunging and welding phases, as a function of the rotational speed. The torque data obtained from the model, for plunging and welding phases, presented a good agreement with the experimental torque data. As shown in Tab. 7, all the relative differences between the torque experimental data and the torque value computed by the model, for both phases, present errors of less than 10%.

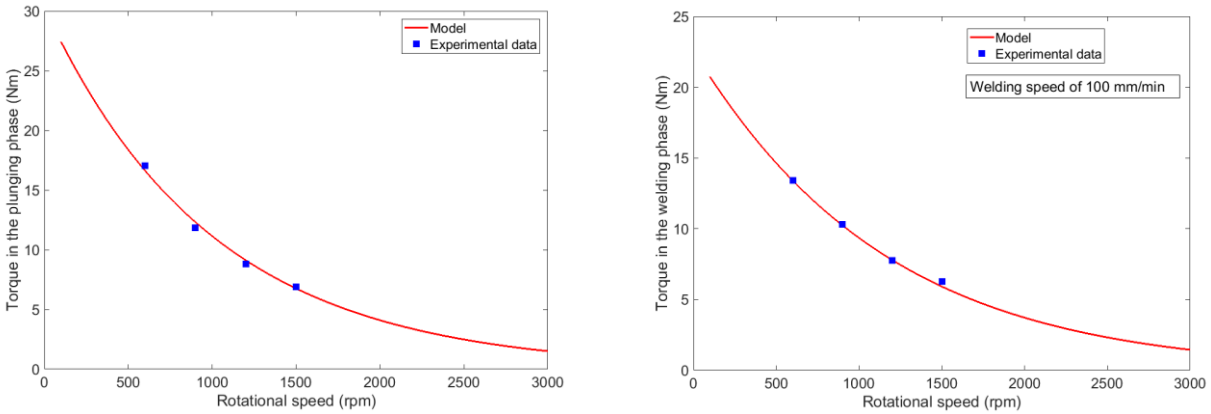

a) b)

Figure 5. Comparison between the torque values obtained experimentally and computed by the model for a) the plunging phase and b) the welding phase.

Tabela 7. Relative differences between the torque data obtained experimentally and the torque computed by the model for the plunging and welding phases.

Rotational speed (rpm)	Welding speed (mm/min)	Relative differences (%)
Plunging phase		
600	----	2.51
900		3.89
1200		3.09
1500		1.71
Welding phase		
600	100	0.00
900		0.62
1200		0.49
1500		5.56
600	200	9.83
900		5.65
1200		2.94
1500		4.31
600	300	2.74
900		0.88
1200		0.84

1500		5.50

5. CONCLUSIONS

The influence of the tool pin and tool shoulder on the torque was analyzed separately by means of the experimental data obtained for several combinations of tool geometry types and rotational, plunging, and welding speeds. Based on the experimental results and on the physical phenomena of the FSW process, a mechanistic model was presented to describe the torque contribution for the complete tool.

The highest torque value was observed in the plunging phase; therefore, the plunging is the critical phase and the factors that influenced the critical torque value are the tool geometry and the plunging and rotational speeds.

The pin of the tool is the part that makes the first contact with the material and together with the rotational and plunging speeds provides the heat input to soften the material. Therefore, the pin has a significant influence on the torque and with an adequate design the critical torque in the process can be reduced.

During the plunging phase, the analysis of variance indicated that there is an interaction between the effects of rotational and plunging speeds on the torque, suggesting that the influence of these factors must be analyzed together. However, the torque is mainly influenced by the rotational speed. For a tool composed only by pin and for a complete tool, the torque value decreases exponentially with the rotational speed and, for a tool composed only by shoulder, the torque decreases logarithmically with the rotational speed while, for all cases, the torque presents a slight increase with the increment of the plunging speed.

During the welding phase, the variance analysis indicated that there exists an interaction between the effects of the rotational and welding speeds on the torque, suggesting that the influence of these factors on the torque must be analyzed together. The results showed that the torque also decreases exponentially with the increase of the rotational speed while it presents a slight increase with the increase of the welding speed.

The torque model for the plunging and welding phases presented a good agreement with the torque experimental data. The model considers the contributions of the local shear yield stress, the tool geometry, and the rotational, plunging, and welding speeds.

6. ACKNOWLEDGEMENTS

This work was partially supported by CAPES, the Brazilian Federal Agency for Support and Evaluation of Graduate Education; CNPq, the Brazilian National Council for Scientific and Technological Development and FAPERJ, the Foundation for Research Support of the State of Rio de Janeiro, Brazil.

7. REFERENCES

Cui, S., Chen, Z.W., Robson, J.D., 2010, “A Model Relating Tool Torque and Its Associated Power and Specific Energy to Rotation and Forward Speeds During Friction Stir welding/Processing”, Int. J. Mach. Tools Manuf., Vol. 50, No. 12, pp. 1023-1030.

Hussein, S.A., Tahir, A.S.M., Izamshah, R., 2015, “Generated Forces and Heat During the Critical Stages of Friction Stir Welding and Processing”, J. Mech. Sci. Technol., Vol. 29, No. 10, pp. 4319-4328.

Khandkar, M., Khan, J., Reynolds, A., 2003, “Prediction of Temperature Distribution and Thermal History During Friction Stir Welding: Input Torque Based Model”, Sci. Technol. Weld. Joining, Vol. 8, No. 3, pp. 165-174.

Kumar, R., Singh, K., Pandey, S., 2012, “Process forces and heat input as function of process parameters in AA5083 friction stir welds”, Trans. Nonferrous Met. Soc. China, Vol. 22, No. 2, pp. 288-298.

Long, T., Tang, W., Reynolds, A., 2007, “Process Response Parameter Relationships in Aluminium Alloy Friction Stir Welds”, Sci. Technol. Weld. Joining, Vol. 12, No. 4, pp. 311-317.

Mahoney, M.W., Rhodes, C.G., Flintoff, J.G., Spurling, R.A., Bingel, W.H., 1998, “Properties of Friction-Stir-Welded 7075 T651 Aluminum”, Metall. Mater. Trans. A, Vol. 29, No. 7, pp. 1955-1964.

Mishra, R.S. and Ma, Z.Y., 2005 “Friction Stir Welding and Processing”, Mater. Sci. Eng. R, Vol. 50, No. 1-2, pp. 1-78.

Nandan, R., Debroy, T., Bhadeshia, H.K.D.H., 2008, “Recent advances in friction-stir welding-Process, weldment structure and properties”, Prog. Mater. Sci., Vol. 53, No. 6, pp. 980-1023.

Pew, J.W., Nelson, T.W., Sorensen, C.D., 2007, “Torque Based Weld Power Model for Friction Stir Welding”, Sci. Technol. Weld. Joining, Vol. 12, No. 4, pp. 341-347.

Qian, J., Li, J., Sun, F., Xiong, J., Zhang, F., Lina, X., 2013, “An Analytical Model to Optimize Rotation Speed and Travel Speed of Friction Stir Welding for Defect-Free Joints”, Scr. Mater. Vol. 68, No. 3-4, pp. 175-178.

Quintana, K.J., Silveira, J.L., 2017a, “Analysis of Torque in Friction Stir Welding of Aluminum Alloy 5052 by Inverse Problem Method”, ASME J. Manuf. Sci. Eng., Vol. 139, No. 4, pp. 041017.

Quintana, K.J., Silveira, J.L., 2017b, "Mechanistic models and experimental analysis for the torque in FSW considering the tool geometry and the process velocities", J. Manuf. Process., Vol. 30, pp. 406-417.

Quintana, K.J., Silveira, J.L., 2018, "Mechanistic models for the forces in FSW of aluminum alloy 5052-H34", Int. J. Advan. Manuf. Technol., available online. https://doi.org/10.1007/s00170-018-1859-3

Rajakumar, S., Muralidharan, C., Balasubramanian, V., 2011, "Statistical Analysis to Predict Grain Size and Hardness of the Weld Nugget of Friction Stir Welded AA6061-T6 Aluminium Alloy Joints", Int. J. Adv. Manuf. Technol., Vol. 57, No. 1, pp. 151-165.

Rhodes, C.G., Mahoney, M.W., Bingel, W.H., Spurling, R.A., Bampton, C.C., 1997, "Effects of Friction Stir Welding on Microstructure of 7075 Aluminum", Scr. Mater. Vol. 36, No. 1, pp. 69-15.

Schmidt, H., Hattel, J., Wert, J., 2004, "An Analytical Model for the Heat Generation in Friction Stir Welding", Modell. Simul. Mater. Sci. Eng., Vol. 12, No. 1, pp. 143-157.

Upadhyay, P., Reynolds, A.P., 2010, "Effects of Thermal Boundary Conditions in Friction Stir Welded AA7050-T7 Sheets", Mater. Sci. Eng. A, Vol. 527, No. 6, pp. 1537-1543.

Yan, J., Sutton, M., Reynolds, A., 2005, "Process–Structure–Property Relationships for Nugget and Heat Affected Zone Regions of AA2524–T351 Friction Stir Welds", Sci. Technol. Weld. Joining, Vol. 10, No. 6, pp. 725-736.

8. AUTHOR'S RESPONSIBILITY

"The authors are the only responsible for the content of this work."